Clim. Past Discuss., 11, 3937–3971, 2015
www.clim-past-discuss.net/11/3937/2015/
doi:10.5194/cpd-11-3937-2015
© Author(s) 2015. CC Attribution 3.0 License.

Climate of the Past Discussions

This discussion paper is/has been under review for the journal Climate of the Past (CP).
Please refer to the corresponding final paper in CP if available.

Laurentide Ice Sheet basal temperatures at the Last Glacial Cycle as inferred from borehole data

C. Pickler[1], H. Beltrami[2,3], and J.-C. Mareschal[1]

[1]GEOTOP, Centre de Recherche en Géochimie et en Géodynamique, Université du Québec à Montréal, Canada
[2]Climate & Atmospheric Sciences Institute and Department of Earth Sciences, St. Francis Xavier University, Antigonish, Nova Scotia, Canada
[3]Centre ESCER pour l'étude et la simulation du climat à l'échelle régionale, Université du Québec à Montréal, Canada

Received: 25 June 2015 – Accepted: 3 August 2015 – Published: 27 August 2015

Correspondence to: H. Beltrami (hugo@stfx.ca)

Published by Copernicus Publications on behalf of the European Geosciences Union.

Abstract

Thirteen temperature-depth profiles (≥ 1500 m) measured in boreholes in eastern and central Canada were inverted to determine the ground surface temperature histories during and after the last glacial cycle. The sites are located in the southern part of the region covered by the Laurentide Ice Sheet. The inversions yield ground surface temperatures ranging from −1.4 to 3.0 °C throughout the last glacial cycle. These temperatures, near the pressure melting point of ice, allowed basal flow and fast flowing ice streams at the base of the Laurentide Ice Sheet. Despite such conditions, which have been inferred from geomorphological data, the ice sheet persisted throughout the last glacial cycle. Our results suggest some regional trends in basal temperatures with possible control by internal heat flow.

1 Introduction

The impact of future climate change on the stability of the present-day ice sheets in Greenland and Antarctica is a major concern of the scientific community (e.g. Gomez et al., 2010; Mitrovica et al., 2009). Satellite gravity measurements performed during the GRACE mission suggest that the mass loss of the Greenland and Antarctic glaciers has accelerated during the decade 2002–2012 (Velicogna and Wahr, 2013). Over the past two decades, mass loss from the Greenland Ice Sheet has quadrupled and contributed to a fourth of global sea level rise from 1992 to 2011 (Church et al., 2011; Straneo and Heimbach, 2013). In 2014, two teams of researchers noted that the collapse of the Thwaites Glacier Basin, an important component holding together the West Antarctic Ice Sheet, was potentially underway (Joughin et al., 2014; Rignot et al., 2014). The collapse of the entire West Antarctic Ice Sheet would lead to rise in sea level by at least 3 m. The present observations of the ice sheet mass balance are important. However, to predict the effects of future climate change on the ice sheets, it is necessary to fully understand the mechanisms of ice sheet growth, decay, and col-

lapse throughout the past glacial cycles. The models of ice sheet dynamics during past glacial cycles show that the thickness and elevation of the ice sheets and the thermal conditions at their base are key parameters controlling the basal flow regime and the evolution of the ice volume (Marshall and Clark, 2002; Hughes, 2009).

During the last glacial cycle (LGC), ~ 120000–12000 years BP, large ice sheets formed in the Northern Hemisphere, covering Scandinavia and almost all of Canada (Denton and Hughes, 1981; Peltier, 2002, 2004; Zweck and Huybrechts, 2005). The growth and decay of ice sheets are governed mainly by ice dynamics and ice sheet-climate interactions (Oerlemans and van der Veen, 1984; Clark, 1994; Clark and Pollard, 1998). Ice dynamics are also strongly controlled by the underlying geological substrate and associated processes (Clark et al., 1999; Marshall, 2005). Clark and Pollard (1998) studied how the ice thickness and the nature of the geological substrate control flow at the base of the glacier. They showed that soft beds, beds of unconsolidated sediment at relatively low relief, result in thin ice sheets that are predisposed to fast ice flow when possible. Hard beds, beds of high relief crystalline bedrock, on the other hand, provide the ideal conditions for the formation of larger, thick ice sheets that experience stronger bed-ice sheet coupling and slow ice flow. Basal flow rate is also affected by the basal temperatures, which play a key role in determining the velocity. However, the ice sheet evolution models use basal temperatures that are poorly constrained because of the lack of direct data pertaining to thermal conditions at the base of ice sheets. The objective of the present study is to use borehole temperature depth data to estimate how the temperatures varied at the base of the Laurentide Ice Sheet during the last glacial cycle.

Temporal variations in ground surface temperatures (GST) are recorded by Earth's subsurface as perturbations to the "steady-state" temperature profile (e.g., Hotchkiss and Ingersoll, 1934; Birch, 1948; Beck, 1977; Lachenbruch and Marshall, 1986). With no changes in GST, the thermal regime of the subsurface is governed by the outflow of heat from Earth's interior resulting in a profile where temperature increases with depth. In homogeneous rocks without heat sources, the "equilibrium temperature" increases

linearly with depth. When changes in ground surface temperature occur and persist, they are diffused downward and recorded as perturbations to the semi-equilibrium thermal regime. These perturbations are superimposed on the temperature-depth profile associated with the flow of heat from Earth's interior. For periodic oscillations of the surface temperature, the amplitude of the temperature fluctuations decreases exponentially with depth over a length scale proportional to the square root of the period ($z \propto \sqrt{\kappa t}$), where κ is the thermal diffusivity of the rock. Long time persistent transients affect subsurface temperature to great depths. Hotchkiss and Ingersoll (1934) were the first to attempt and infer past climate from such temperature-depth profiles, specifically they estimated the timing of the last glacial retreat from temperature measurements in the Calumet copper mine in northern Michigan. Birch (1948) estimated the perturbations to the temperature gradient caused by the last glaciation and suggested a correction to heat flux determinations in regions that had been covered by ice during the LGC. A correction including the glacial-interglacial cycles of the past 400 000 years was proposed by Jessop (1971) to adjust the heat flow measurements made in Canada. It was only in the 1970s that systematic studies were undertaken to infer past climate from borehole temperature profiles (Cermak, 1971; Sass et al., 1971; Beck, 1977). The use of borehole temperature data for estimating recent (< 300 years) climate changes became widespread in the 1980s because of concerns about increasing global temperatures (Lachenbruch and Marshall, 1986; Lachenbruch, 1988). High precision borehole temperature measurements have been mostly made for estimating heat flux in relatively shallow (a few hundred meters) holes drilled for mining exploration. Such shallow boreholes are suitable for studying recent (< 500 years) climate variations and the available data have been interpreted in many regional or global studies (e.g., Bodri and Cermak, 2007; Jaupart and Mareschal, 2011, and references therein). However, very few deep (≥ 1500 m) borehole temperature data are available to study climate variations on the time scale of 10 to 100 kyr. Oil exploration wells are usually a few km deep but are not suitable because the temperature measurements are not made in thermal equilibrium and lack the required precision. Nonetheless a

few deep mining exploration holes have been drilled, mostly in Precambrian Shields, where temperature measurements can be used for climate studies on the time scale of the LGC. In Canada, Sass et al. (1971) measured temperatures in a deep (3000 m) borehole near Flin Flon, Manitoba, and used direct models to show that the surface temperature during the last glacial maximum (LGM), ∼ 20 000 years BP, could not have been more than 5 K colder than present. Other Canadian deep boreholes temperature profiles have since been measured revealing regional differences in temperatures during the LGM. From a deep borehole in Sept-Iles, Québec, Mareschal et al. (1999b) found surface temperatures to be approximately 10 K colder than present. This was confirmed by Rolandone et al. (2003b) who studied four deep holes and suggested that LGM surface temperatures were colder in eastern Canada than in central Canada.

Chouinard and Mareschal (2009) examined eight deep boreholes located from central to eastern Canada and observed significant regional differences in heat flux, temperature anomalies and ground surface temperature histories. On the other hand, studies of deep boreholes in Europe lead to different conclusions for the Fennoscandian Ice Sheet which covered parts of Eurasia during the LGC (e.g., Demezhko and Shchapov, 2001; Kukkonen and Jõeleht, 2003; Demezhko and Gornostaeva, 2015). Kukkonen and Jõeleht (2003) analyzed heat flow variations in the Baltic Shield and the Russian Platform and found a 8 ± 4.5 K temperature increase following the LGM. Demezhko and Shchapov (2001) studied a ∼ 5 km deep borehole in the Urals, Russia, and found a postglacial warming of 12–13 K with basal temperatures below the melting point of ice during the LGM. This was confirmed by recent work indicating that temperatures in the Urals were ∼ −8 °C at the LGM (Demezhko and Gornostaeva, 2015).

In this study, we shall examine all the deep borehole temperature profiles measured in central and eastern Canada in order to determine the temperature at the base of the Laurentide Ice Sheet, which covered the area during the LGC. The geographical extent of the study is confined to the southern portion of the Laurentide Ice Sheet because deep mining exploration boreholes have only been drilled in the southernmost part of the Canadian Shield.

2 Theory

For calculating the temperature-depth profile, we assume that heat is transported only by vertical conduction and that the temperature perturbation is the result of a time-varying, horizontally uniform, surface temperature boundary condition. The temperature at depth in the Earth, for a homogeneous, source-free half space with horizontally uniform variations in the surface temperature, can be written as:

$$T(z) = T_o + Q_o R(z) - \int_0^z \frac{\mathrm{d}z'}{\lambda(z')} \int_0^{z'} H(z'')\mathrm{d}z'' + T_t(z) \tag{1}$$

where T_o is the reference ground surface temperature ("steady-state"/long-term surface temperature), Q_o is the reference heat flux ("steady-state" heat flux from depth), $\lambda(z)$ is the thermal conductivity, z is depth, H is the heat generation, and $T_t(z)$ is the temperature perturbation at depth z due to time-varying changes to the surface boundary condition. $R(z)$ is the thermal resistance to depth z, which is defined as:

$$R(z) = \int_0^z \frac{\mathrm{d}z'}{\lambda(z')} \tag{2}$$

Thermal conductivity is measured on core samples, usually by the method of divided bars (Misener and Beck, 1960). Radiogenic heat production is also measured on core samples. The temperature perturbation at depth z resulting from surface temperature variations can be written as (Carslaw and Jaeger, 1959):

$$T_t(z) = \int_0^\infty \frac{z}{2\sqrt{\pi\kappa t^3}} \exp\left(\frac{-z^2}{4\kappa t}\right) T_o(t)\mathrm{d}t \tag{3}$$

where t is time before present, κ is thermal diffusivity and $T_o(t)$ is the surface temperature at time t (Carslaw and Jaeger, 1959). For a stepwise change ΔT in surface temperature at time t before present, the temperature perturbation at depth z is given by (Carslaw and Jaeger, 1959):

$$T_t(z) = \Delta T \operatorname{erfc}\left(\frac{z}{2\sqrt{\kappa t}}\right) \quad (4)$$

where erfc is the complementary error function.

If the ground surface temperature variation is approximated by a series of constant values ΔT_k during K time intervals (t_{k-1}, t_k), the temperature perturbation can be written as follows:

$$T_t(z) = \sum_{k=1}^{K} \Delta T_k \left(\operatorname{erfc}\frac{z}{2\sqrt{\kappa t_k}} - \operatorname{erfc}\frac{z}{2\sqrt{\kappa t_{k-1}}}\right) \quad (5)$$

The ΔT_k represent the departure of the average GST during each time interval from T_o.

2.1 First order estimate of the GST History

We have directly used variations in the long-term surface temperature with depth to obtain a first order estimate of time variations in surface temperature. To interpret subsurface anomalies as records of GST history variations, we must separate the climate signal from the quasi steady-state temperature profile. The quasi steady-state thermal regime is estimated by a least squares linear fit to the lowermost 100 m section of the temperature-depth profile. The slope and the surface intercept of the fitted line are interpreted as the "steady-state" temperature gradient Γ_o and the long-term surface temperature T_o respectively. The bottom part of the profile is the section least affected by the recent changes in surface temperature and dominated by the steady-state heat flow from Earth's interior. When we are using a shallower section of the profile, the estimated long-term temperature and gradient are more affected by recent perturbations

in the surface temperature. The shallower the section, the more recent the perturbation. Thus we determine how the estimated long-term surface temperature varies with time by iterating through different sections of the temperature-depth profile. Using the scaling of Eq. (4), the time it takes for the surface temperature variation to propagate into the ground and the depth of the perturbations are related by:

$$t \approx z^2/4\kappa \quad (6)$$

with κ thermal diffusivity, z is the depth, and t is time.

This approach yields only a first order estimate because the temperature perturbations are attenuated as they are diffused downward. However, the temporal variation of the long-term surface temperature is obtained by extrapolating the semi-equilibrium profile to the surface. The effect of a small change in gradient on the long-term surface temperature is proportional to the average depth where the gradient is estimated. Variations in the calculated long-term surface temperature are thus less attenuated than the perturbations in the profile and may well provide a gross approximation of the GST history, but independent of the model assumptions in an inversion procedure.

2.2 Inversion

In order to obtain a more robust estimate of the GST histories, we have inverted the temperature-depth profiles for each site and, whenever profiles from nearby sites are available, we have inverted them jointly. The inversion consists of determining T_o, Q_o, and the ΔT_k from the temperature-depth profile (Eq. 5). For each depth where temperature is measured, Eq. (5) yields a linear equation in ΔT_k. For N temperature measurements, we obtain a system of N linear equations with $K+2$ unknowns, T_o, Q_o, and K values of ΔT_k. Even when $N \geq K+2$, the system seldom yields a meaningful solution because it is ill-conditioned. This means that the solution is unstable and a small error in the data results in a very large error in the solution (Lanczos, 1961). Different authors have proposed different inversion techniques to obtain the GST history from the data (e.g., Vasseur et al., 1983; Shen and Beck, 1983; Nielsen and Beck, 1989; Wang,

1992; Shen and Beck, 1991; Mareschal and Beltrami, 1992; Clauser and Mareschal, 1995; Mareschal et al., 1999b). Here, to obtain a "solution" regardless of the number of equations and unknowns and to reduce the impact of noise and errors on this solution, singular value decomposition is used (Lanczos, 1961; Jackson, 1972; Menke, 1989). This technique is well documented and further details can be found in Mareschal and Beltrami (1992); Clauser and Mareschal (1995); Beltrami and Mareschal (1995); Beltrami et al. (1997).

2.3 Simultaneous inversion

As meteorological trends remain correlated over a distance on the order of 500 km (Beltrami et al., 1997), boreholes within the same region are assumed to have been affected by the same surface temperature variations and their subsurface temperature anomalies are expected to be consistent. This holds only if the surface conditions are identical for all boreholes. If these conditions are met, jointly inverting different temperature-depth profiles from the same region will increase the signal to noise ratio. Singular value decomposition was used to jointly invert the sites with multiple boreholes. A detailed description and discussion of the methodology can be found in papers by Beltrami and Mareschal (1995) and Beltrami et al. (1997).

3 Data Description

We have used thirteen deep boreholes ($\geq$ 1500 m) across eastern and central Canada to determine the temperature throughout and after the LGC. All the sites are located in the southern portion of the Canadian Shield, which was covered by the Laurentide Ice Sheet that extended over most of Canada during the LGC (Fig. 1). Borehole locations and depths are summarized in Table 1. Detailed description of the measurement techniques as well as the relevant geological information can be obtained from the heat

flow studies (Sass et al., 1971; Mareschal et al., 1999b, a; Rolandone et al., 2003a, b; Perry et al., 2006, 2009; Jaupart et al., 2014).

A description of eight sites, Flin Flon, Pipe, Manitouwadge 0610, Manitouwadge 0611, Balmertown, Falconbridge, Lockerby, and Sept Iles, can be found in Rolandone et al. (2003b) and Chouinard and Mareschal (2009). Five additional profiles (Owl, near Thompson, Manitoba, Victor and Craig Mines both near Sudbury, Ontario, Matagami and Val d'Or, Québec) were analyzed. The Val d'Or borehole was logged in 2010 to a depth of ~1750 m. It is situated 15 km east of the mining camp of Val d'Or, Québec in a flat forested area. The Matagami borehole is located near the mining camp of Matagami, some 300 km north of Val d'Or. The Owl borehole, which was logged in 1999 and 2001, is located ~5 km from the Birchtree Mine and ~8 km south of the city of Thompson, Manitoba. The two other new boreholes, Craig Mine and Victor Mine, are located within the Sudbury structure, north-east of Lake Huron, in Ontario. The Craig Mine borehole, near the town of Levack, north-west of Sudbury, was logged in 2004. The deep mine was in operation when measurements were made and pumping activity was continuous to keep the deep mine galleries from flooding. The Victor Mine site was sampled in 2013, close to the community of Skead, north-east of Sudbury, Ontario. Victor Mine operated in 1959 and 1960 but exploration and engineering work is presently underway to prepare for reopening the mine at greater depth.

We found systematic variations of thermal conductivity at Flin Flon, Thompson (Owl), and Matagami, and we corrected accordingly (Bullard, 1939). We calculated the thermal resistance and obtained a temperature vs. thermal resistance profile that is almost linear. We calculated the heat flux as the slope of the temperature-resistance and found no discontinuity in heat flux along the profile (Table 1). For all the other sites that show no systematic variations in conductivity, we have used the mean thermal conductivity to calculate heat flux. Heat production was measured and found to only be significant at two sites, Lockerby (3 $\mu W\,m^{-3}$) and Victor Mine (0.9 $\mu W\,m^{-3}$), and therefore only taken into account at these sites. In absence of heat production and in steady-state, the heat flux does not vary with thermal resistance. Variations in heat flux with thermal

resistance (or depth) is thus a diagnostic of departure from 1-D steady-state thermal regime. A decrease in heat flux toward the surface is associated with surface warming and enhanced heat flux is due to cooling. The heat flux profiles that we have calculated for all the sites (Fig. 2) exhibit clear departures from 1-D steady-state condition. Most of the profiles show a very pronounced increase of heat flux with depth at shallow depth (<200 m) and a clear trend of increasing heat flux between 500 and 1500 m. The increase at shallow depth is related to very recent (< 300 years) climate warming. The trend between 500 and 1500 m is the result of the surface warming that followed the glacial retreat at ca. 10 ka.

4 Analysis and Results

4.1 Long-term Surface Temperatures

Estimated long-term surface temperatures as a function of time and depth (i.e. $\propto$ depth squared) were determined for each borehole (Fig. 3). The time in these plots represents the time it took the signal to propagate and not the time that the surface temperature perturbation occurred. The range of long-term surface temperatures for each borehole was estimated over its sampled depth and reveal the persistent long-term climate trends. These trends are the mirror image of the heat flow trends.

A decreasing temperature trend with time and depth is apparent in all the boreholes in Manitoba except Pipe that does not show a clear trend. Variations of surface temperature are not consistent, with almost no trend at Pipe and a weak signal at Owl. The Flin Flon borehole is the deepest available for this study and provides a history four times longer than that of the two shallower boreholes at Owl and Pipe. It is consistent with a colder period coinciding with the LGM. In western Ontario, Manitouwadge 0611 exhibits very strong oscillations at depth. The source of noise is difficult to ascertain because of the complicated geological structure and the absence of thermal conductivity data. Borehole 0610 at Manitouwadge is consistent with colder tempera-

tures during the LGM but the Balmertown hole does not show any variation in long-term surface temperature. Four profiles at Sudbury, are consistent with colder temperature during the LGM, but the amplitude of the trend varies between sites. Similar trends are observed for the three easternmost holes in Québec with long-term temperatures on average 5 K lower near the bottom of the holes than near the surface.

These first order estimates suggest colder surface temperatures during the LGM at most of the sites. In order to better quantify the surface temperature changes, we must turn to inversion and obtain the GST histories.

4.2 Individual inversions

The GST histories at all the studied sites for the time period of 100 to 100 000 years BP was inverted from the temperature-depth profiles. The time span of the GST history model consists of 16 intervals whose distribution varies logarithmically because the resolution decreases with time. A singular value cutoff of 0.08 was used for all the individual profile inversions (Figs. 4–7). A summary of the inversion results can be found in Table 2. Two main episodes can be recognized in the GST histories: One is associated with a minimum temperature that occurred around the LGM at ca. 20 ka. The second is a warming observed at ca. 2–6 ka coinciding with the Holocene Climatic Optimum (HCO), a warm period that followed the deglaciation (Lamb, 1995).

For the purpose of the discussion, we have grouped the sites sites that are from the same geographical region. We shall thus distinguish between Manitoba, western Ontario, the Sudbury area, and Québec.

The sites from Manitoba, Flin Flon, Owl and Pipe, have not recorded a very strong signal (Fig. 4). This may be in part because the present ground surface temperature is very low; it is close to 0 °C in Thompson where intermittent permafrost is found. At Flin Flon, where the present ground temperature is near 3 °C, ground temperature variations were small. The surface temperature was minimum around the LGM and was near the melting point of ice (−0.3 °C). For Pipe, little to no signal was recorded. We found that there was minimal change in the ground surface temperature (~ 2.5 K

in amplitude) over the past 100,000 years. For Owl, the amplitude of the temperature changes has doubled (~5 K), with the minimum temperature (−2.4 °C) around the LGM and a warming around the HCO. Although this result is plausible, some uncertainty remains as Guillou-Frottier et al. (1996) noted high heat flux correlated with high thermal conductivity in the Thompson Belt. The elevated thermal conductivity is due to the presence of vertical slices of quartzites, which increase thermal conductivity by a factor of 1.7. Furthermore, the site is affected by a poorly resolved conductivity structure as thermal conductivity measurements vary in the deepest part of the borehole, between 2.21 and 5.14 $W m^{-1} K^{-1}$. The lateral heat refraction effects due to the thermal conductivity contrast affect the temperature profiles and alter the GST history. For these reasons, we have little confidence in the robustness of the Owl GST history reconstruction.

In western Ontario (Balmertown, Manitouwadge 0610, and 0611), results at all sites show minimum temperatures around the LGM, with a very weak minimum at Balmertown (Fig. 5). However, the amplitude of the temperature change is much larger at Manitouwadge 0611 (~10 K) than Balmertown (~2 K) and Manitouwadge 0610 (~3 K). As the two Manitouwadge sites are only ~40 km apart, this difference is surprising. While Manitouwadge 0611 yields a plausible GST history, it appears to have an amplified signal. The site is located in a complex geological structure and lacks thermal conductivity data. There is also a change in the temperature gradient at 500 m, which cannot be accounted for. In the absence of thermal conductivity data, we cannot consider the GST history for Manitouwadge 0611 as reliable.

All four sites in the Sudbury region, Craig Mine, Falconbridge, Lockerby, and Victor Mine, have recorded minimal temperatures around the LGM (Fig 6). However, the minimum past temperatures for the region do vary between sites. The coldest minimum temperature occurs at Craig Mine. The amplitude of the temperature changes for the site (~12 K) is much larger than those of the other sites, which vary between ~5–7 K. This difference is unexpected as these sites are all within the Sudbury craton and should have recorded similar histories. The Craig Mine signal appears amplified, which could be the result of water flows induced by pumping at levels below 2000 m in

the mine. We thus believe that the GST history for Craig Mine is not reliable. The minimum temperatures at Lockerby and Victor Mine, 2.8 and 3.0 °C, are also the highest of the study. These are also the only two sites with non-negligible heat production, 3 and 0.9 $\mu W m^{-3}$ respectively. The corrections for heat production produce an increase of the temperature gradient proportional to depth and result in an amplification of the warming signal in the profile. Consequently, the minimum and maximum temperatures would be higher at these sites, Lockerby and Victor Mine, than those with negligible heat production.

The GST histories from the three boreholes in Québec, Matagami, Val d'Or and Sept Iles, display regional differences (Fig. 7). However, their minimum temperatures all occur around the LGM. The lowest minimum temperature occurred in this region, −1.4 °C at Sept Iles.

At all sites, excluding Pipe, there is warming following the LGM that can be associated with the HCO, a warm period whose maximal temperatures have been dated at 4.4–6.8 ka with palynological reconstructions from northern Ontario and northern Michigan (Boudreau et al., 2005; Davis et al., 2000).

We have compared the ranges of temperature in the inverted GST histories with those of the long-term surface temperature variations for all the sites (Table 4). Although the total range varies between sites from ~2 to ~8 K, the two methods yield consistent values that differ by less than 1 K at most of the sites. The warming trend in the long-term surface temperature variations is consistent with the inverted GST histories. This correlation between the long-term surface temperature ranges and the persistent long-term GST history trends suggests that our results are robust. All the long-term surface temperature variations exhibit short period oscillations that are not present in the GST histories and do not clearly show the presence of the HCO. These oscillations could explain the discrepancy between the temperature ranges of the inverted GST histories and that of the long-term surface temperature variations for Flin Flon and Pipe.

4.3 Simultaneous Inversion

We have inverted simultaneously the boreholes of Thompson (Owl and Pipe), Manitouwadge (0610 and 0611) and Sudbury (Craig Mine, Falconbridge, Lockerby, and Victor Mine) to observe regional trends and to improve the signal to noise ratio (Fig. 8). For simultaneous inversion, the temperature-depth profiles were truncated to ensure a common depth for all the boreholes. This facilitates comparison and means that we are examining the subsurface temperature anomalies for the same time period. For all inversions, the minimum temperature occurs around the LGM and are followed by a warming associated with the HCO. While Owl and Manitouwadge 0611 have questionable individual inversions, the regions of Thompson and Manitouwadge are still simultaneously inverted in an attempt to decrease the signal to noise ratio. For Thompson, the amplitude of the GST history temperature range is ~ 4 K. As Pipe did not appear to record a signal, the simultaneous inversion appears to have damped slightly the questionable signal recorded at Owl. The amplitude difference for the Manitouwadge GST history is ~8 K, between that of 0610 (~ 3 K) and 0611 (~ 10 K).

The Sudbury simultaneous inversion was done with and without Craig Mine. This was done to see whether the inclusion of Craig Mine, a site which is likely to have been affected by water flow, affects the reconstructions. Both inversions display similar trends, however, the differences lie in the amplitude variations. The inversion excluding Craig Mine yielded a ΔT of 7 K, similar to those of the individual inversions of Falconbridge (~ 7 K), Lockerby (~ 7 K) and Victor Mine (~ 5 K). Upon inclusion of Craig Mine, ΔT increased by 4 K, demonstrating the amplification effect of the site.

5 Discussion

The minimum temperatures of the GST histories occur around the LGM, representing the basal temperatures of the Laurentide Ice Sheet. These temperatures vary spatially and range from -1.4 – 3.0^{o}C, near the pressure melting point of ice. This spatial variation is expected as numerous studies have demonstrated present-day spatial basal temperature variability beneath the Antarctic and Greenland Ice Sheets (e.g., Dahl-Jensen et al., 1998; Pattyn, 2010; Schneider et al., 2006). The highest basal temperatures occur within the Sudbury basin at Lockerby and Victor Mine. The region has the highest average heat flux of the Canadian Shield, $\sim 54\, mW\, m^{-2}$, implying higher than average crustal heat production (Perry et al., 2009). The lowest basal temperature is recorded at Sept Iles, a region with the lowest heat flux of the studied regions, $\sim 34\, mW\, m^{-2}$. These correlations suggest a link between heat flux and basal temperatures. This is further supported by modelling work showing heat flux influences the thermal structure and properties of ice sheets, including basal temperatures and flow (Pollard et al., 2005). However, the Sept Iles basal temperature has been linked to its proximity to the edge of the ice sheet and area of thinner ice (Rolandone et al., 2003b). Our studies support a possible link between basal temperature and heat flux along with ice dynamics in the Laurentide Ice Sheet during the LGC but further modelling work is necessary to confirm such a relationship. Variations in these parameters (heat flux and ice dynamics) could account for the differences observed in the basal temperatures of the Fennoscandian and Laurentide ice sheets.

The basal temperatures recorded, near the pressure melting point of ice, indicate the possibility of basal flow and ice streams, two important factors affecting ice sheet evolution. These processes have been suggested by geomorphological evidence presented by Dyke et al. (2002) and predicted by the ICE-5G model (Peltier, 2004). Basal flow has the ability to transport large amounts of water from the interior of the ice sheet, leading to thinning of the ice sheet and climatically-vulnerable ice. It is postulated to be a key factor in glacial terminations (Marshall and Clark, 2002). Furthermore, these temperatures demonstrate that the southern portion of the Laurentide Ice Sheet was not frozen to the bed, suggesting basal sliding. These conditions can lead to instability. Widespread basal sliding and increase surface meltwater could have been a factor resulting in the rapid collapse of the Laurentide Ice Sheet (Zwally et al., 2002). However, these basal temperatures and associated melt persisted prior to and throughout the

LGM over more than 30 000 years with deglaciation only occurring rapidly during the early Holocene (Carlson et al., 2008). While this indicates that basal temperatures near the pressure melting point of ice cannot be solely responsible for ice sheet instability and collapse, it demonstrates that they are a key parameter in ice sheet evolution, one that ice sheet evolution models must take into account. Elevated basal temperatures, near or above the pressure melting point of ice, have been recorded in the present-day ice sheets (Fahnestock et al., 2001; Pritchard et al., 2012). Our results indicate that alone this cannot be considered as an indication of ice sheet collapse. However, combined with other processes it could lead to instability and collapse.

6 Conclusions

Thirteen deep boreholes from eastern and central Canada were analyzed to determine the GST histories for the last 100 kyr. The long term trends are consistent between sites. A warm period following the retreat of the ice sheet is inferred at ∼2–6 ka in the inverted GST histories, correlated to the Holocene Climatic Optimum.

The surface temperatures reached their minima during the LGM and post glacial warming started ca. 10 ka. The corresponding temperatures at the base of of the Laurentide Ice Sheet range from −1.4 to 3.0 °C, and are all near or above the pressure melting point of ice. Such temperatures allow for basal flow and fast flowing ice streams, two important factors affecting ice sheet evolution, illustrating the need for models of ice sheet evolution to account for such a key parameters as basal temperature. Despite the suggestion that melting took place at its base, the Laurentide ice sheet persisted throughout the LGM over more than 30 000 years. This demonstrates that basal temperatures near the melting point of ice do not indicate that an ice sheet is on the verge of collapse. However, combined with other processes it could lead to instability and collapse.

The differences between GST histories at different sites raise other questions concerning the controls on temperatures at the base of ice sheets. Equilibrium between

heat flow from the Earth's interior and heat advection by glacial flow determines the temperature at the boundary between the ice and the bedrock. The correlation between higher heat flux and higher basal temperatures in the Sudbury region suggests that variations in crustal heat flux might account for some of the regional differences in basal temperatures along with the dynamics of ice thickness controlled by the accumulation rate and the distance to the edge of the ice sheet.

It is also noteworthy that similar deep borehole studies in Europe suggest that basal temperatures beneath the Fennoscandian Ice Sheet during the LGC were much colder than those observed in Canada (Perry et al., 2006). Because of the geological similarities between the two regions, this contrast is likely to be due to differences in climate and ice dynamics between Europe and North America during the LGC.

Acknowledgements. This work was supported by grants from the Natural Sciences and Engineering Research Council of Canada Discovery Grant (NSERC-DG, 140576948), a NSERC-CREATE award Training Program in Climate Sciences, the Atlantic Computational Excellence Network (ACEnet), and the Atlantic Canada Opportunities Agency (AIF-ACOA) to HB. H. Beltrami holds a Canada Research Chair. C.Pickler is funded by a NSERC-CREATE Training Program in Climate Sciences based at St.Francis Xavier University.

References

Beck, A.: Climatically perturbed temperature gradient and their effect on regional and continental heat-flow means, Tectonophysics, 41, 17–39, 1977. 3939, 3940

Beltrami, H. and Mareschal, J.: Resolution of ground temperautre histories inverted from borehole temperature data, Global Planet. Change, 11, 57–70, 1995. 3945

Beltrami, H., Cheng, L., and Mareschal, J. C.: Simultaneous inversion of borehole temperature data for determination of ground surface temperature history, Geophys. J. Int., 129, 311–318, 1997. 3945

Birch, A. F.: The effects of Pleistocene climatic variations upon geothermal gradients, Am. J. Sci., 246, 729–760, 1948. 3939, 3940

Bodri, L. and Cermak, V.: Borehole Climatology, Elsevier, Amsterdam, 2007. 3940

Boudreau, R., Galloway, J., Patterson, R., Kumar, A., and Michel, F.: A paleolimnological record of Holocene climate and environmental change in the Temagami region, northeastern Ontario, J. Paleolimnol., 33, 445–461, 2005. 3950
Bullard, E.: Heat Flow in South Africa, P. R. Soc. Lon. A, 173, 474–592, 1939. 3946
Carlson, A. E., LeGrande, A. N., Oppo, D. W., Came, R. E., Schmidt, G. A., Anslow, F. S., Licciardi, J. M., and Obbink, E. A.: Rapid early Holocene deglaciation of the Laurentide ice sheet, Nat. Geosci., 1, 620–624, 2008. 3953
Carslaw, H. and Jaeger, J.: Conduction of Heat in Solids, Oxford Science Publications, New York, 550 pp., 1959. 3942, 3943
Cermak, V.: Underground temperature and inferred climatic temperature of the past millenium, Palaeogeogr. Palaeoecol., 10, 1–19, 1971. 3940
Chouinard, C. and Mareschal, J.-C.: Ground surface temperature history in southern Canada: Temperatures at the base of the Laurentide ice sheet and during the Holocene, Earth Planet. Sci. Lett., 277, 280–289, doi:10.1016/j.epsl.2008.10.026, 2009. 3941, 3946, 3960
Church, J. A., White, N. J., Konikow, L. F., Domingues, C. M., Cogley, J. G., Rignot, E., Gregory, J. M., van den Broeke, M. R., Monaghan, A. J., and Velicogna, I.: Revisiting the Earth's sea-level and energy budgets from 1961 to 2008, Geophys. Res. Lett., 38, doi:10.1029/2011GL048794, 2011. 3938
Clark, P. U.: Unstable behavior of the Laurentide Ice Sheet over deforming sediment and its implications for climate change, Quaternary Res., 41, 19–25, 1994. 3939
Clark, P. U. and Pollard, D.: Origin of the Middle Pleistocene Transition by ice sheet erosion of regolith, Paleoceanography, 13, 1–9, 1998. 3939
Clark, P. U., Alley, R. B., and Pollard, D.: Northern Hemisphere Ice-Sheet Influences on Global Climate Change, Science, 286, 1104–1111, 1999. 3939
Clauser, C. and Mareschal, J.-C.: Ground temperature history in central Europe from borehole temperature data, Geophys. J. Int., 121, 805–817, 1995. 3945
Dahl-Jensen, D., Mosegaard, K., Gundestrup, N., Clow, G. D., Johnsen, S. J., Hansen, A. W., and Balling, N.: Past Temperatures Directly from the Greenland Ice Sheet, Science, 282, 268–271, 1998. 3952
Davis, M., Douglas, C., Calcote, R., Cole, K., Green Winkler, M., and Flakne, R.: Holocene climate in the Western Great Lakes national park and lakeshores: implications for future climate change, Conserv. Biol., 14, 968–983, 2000. 3950

Demezhko, D. Y. and Gornostaeva, A. A.: Late Pleistocene-Holocene ground surface heat flux changes reconstructed from borehole temperature data (the Urals, Russia), Clim. Past, 11, 647–652, doi:10.5194/cp-11-647-2015, 2015. 3941
Demezhko, D. and Shchapov, V.: 80 000 years ground surface temperature history inferred from the temperature-depth log measured in the superdeep hole SG-4 (the Urals, Russia), Global Planet. Change, 20, 219–230, 2001. 3941
Denton, G. and Hughes, T., eds.: The Last Great Ice Sheets, Wiley-Interscience, New York, 1981. 3939
Dyke, A., Andrews, J., Clark, P., England, J., Miller, G., Shaw, J., and Veillette, J.: The Laurentide and Innuitian ice sheets during the Last Glacial Maximum, Quatern. Sci. Rev., 21, 9–31, doi:10.1016/S0277-3791(01)00095-6, 2002. 3952
Gomez, N., Mitrovica, J. X., Tamisiea, M. E., and Clark, P. U.: A new projection of sea level change in response to collapse of marine sectors of the Antarctic Ice Sheet, Geophys. J. Int., 180, 623–634, 2010. 3938
Guillou-Frottier, L., Jaupart, C., Mareschal, J. C., Gariépy, C., Bienfait, G., Cheng, L. Z., and Lapointe, R.: High heat flow in the trans-Hudson Orogen, Central Canadian Shield, Geophys. Res. Lett., 23, 3027–3030, doi:10.1029/96GL02895, 1996. 3949
Hotchkiss, W. and Ingersoll, L.: Post-glacial time calculations from recent geothermal measurements in the Calumet Copper Mines, J. Geol., 42, 113–142, 1934. 3939, 3940
Hughes, T.: Modeling ice sheets from the bottom up, Quatern. Sci. Rev., 28, 1831–1849, 2009. 3939
Jackson, D.: Interpretation of inaccurate, insufficient, and inconsistent data, Geophys. J. Int., 28, 97–110, 1972. 3945
Jaupart, C. and Mareschal, J.-C.: Heat generation and transport in the Earth, Cambridge University Press, 357–379, 2011. 3940
Jaupart, C., Mareschal, J., Bouquerel, H., and Phaneuf, C.: The building and stabilization of an Archean Craton in the Superior Province, Canada, from a heat flow perspective, J. Geophys.l Res.-Solid Earth, 119, 9130–9155, 2014. 3946, 3960
Jessop, A.: The Distribution of Glacial Perturbation of Heat Flow in Canada, Can. J. Earth Sci., 8, 162–166, 1971. 3940
Joughin, I., Smith, B., and Medley, B.: Marine Ice Sheet Collapse Potentially Under Way for the Thwaites Glacier Basin, West Antarctica, Science, 344, 735–738, 2014. 3938

Kukkonen, I. T. and Jõeleht, A.: Weichselian temperatures from geothermal heat flow data, J. Geophys. Res.-Solid Earth, 108, doi:10.1029/2001JB001579, 2003. 3941
Lachenbruch, A. and Marshall, B.: Changing climate: Geothermal evidence from permafrost in the Alaskan Arctic, Science, 234, 689–696, 1986. 3939, 3940
Lachenbruch, A. H.: Permafrost, the active layer and changing climate, Global Planet. Change, 29, 259–273, 1988. 3940
Lamb, H.: Climate, History and the Modern World, Routledge, 2 edn., 114 pp., 1995. 3948
Lanczos, C.: Linear Differential Operators, D. Van Nostrand, Princeton, N. J., 1961. 3944, 3945
Mareschal, J.-C. and Beltrami, H.: Evidence for recent warming from perturbed geothermal gradients: examples from eastern Canada, Clim. Dynam., 6, 135–143, doi:10.1007/BF00193525, 1992. 3945
Mareschal, J. C., Jaupart, C., Cheng, L. Z., Rolandone, F., Gariépy, C., Bienfait, G., Guillou-Frottier, L., and Lapointe, R.: Heat flow in the Trans-Hudson Orogen of the Canadian Shield: Implications for Proterozoic continental growth, J. Geophys. Res., 104, 7–29, 1999a. 3946, 3960
Mareschal, J.-C., Rolandone, F., and Bienfait, G.: Heat flow variations in a deep borehole near Sept-Iles, Québec, Canada: Paleoclimatic interpretation and implications for regional heat flow estimates, Geophys. Res. Lett., 26, 2049–2052, doi:10.1029/1999GL900489, 1999b. 3941, 3945, 3946, 3960
Marshall, S.: Recent advances in understanding ice sheet dynamics, Earth Planet. Sci. Lett., 240, 191–204, 2005. 3939
Marshall, S. and Clark, P.: Basal tempeature evolution of North American ice sheets and implications for the 100-kyr cycle, Geophys. Res. Lett., 29, 67–1–67–4, 2002. 3939, 3952
Menke, W.: Geophysical Data Analysis: Discrete Inverse Theory, vol. 4, Academic Press, San Diego, 1989. 3945
Misener, A. and Beck, A.: The measurement of heat flow over land, Interscience, New York, 11–60, 1960. 3942
Mitrovica, J. X., Gomez, N., and Clark, P. U.: The Sea-Level Fingerprint of West Antarctic Collapse, Science, 323, 753–753, 2009. 3938
Nielsen, S. and Beck, A.: Heat flow density values and paleoclimate determined from stochastic inversion of four temperature-depth profiles from the Superior Province of the Canadian Shield, Tectonophysics, 164, 345–359, doi:10.1016/0040-1951(89)90026-7, 1989. 3944

Oerlemans, J. and van der Veen, C.: Ice Sheets and Climate, D. Reidel Publishing Company, Dordrecht, Boston, Lancaster, 1984. 3939
Pattyn, F.: Antarctic subglacial conditions inferred from a hybrid ice sheet/ice stream model, Earth Planet. Sci. Lett., 295, 451–461, 2010. 3952
Peltier, W.: Global glacial isostasy and the surface of the ice-age Earth: The ICE-5G (VM2) Model and GRACE, Annu. Rev. Earth Planet. Sci., 32, 111–149, doi:10.1146/annurev.earth.32.082503.144359, 2004. 3939, 3952
Peltier, W. R.: Global glacial isostatic adjustment: palaeogeodetic and space-geodetic tests of the ICE-4G (VM2) model, J. Quatern. Sci., 17, 491–510, doi:10.1002/jqs.713, 2002. 3939
Perry, H., Jaupart, C., Mareschal, J., and Bienfait, G.: Crustal heat production in the Superior Province, Canadian Shield, and in North America inferred from heat flow data, J. Geophys. Res.-Solid Earth, 111, 2006. 3946, 3954
Perry, H., Mareschal, J. C., and Jaupart, C.: Enhanced crustal geo-neutrino production near the Sudbury Neutrino Observatory, Ontario, Canada, Earth Planet. Sci. Lett., 288, 301–308, 2009. 3946, 3952, 3960
Pollard, D., DeConto, R., and Nyblabe, A.: Sensitivity of Cenozoic Antarctic ice sheet variations to geothermal heat flux, Global Planet. Change, 49, 63–74, 2005. 3952
Rignot, E., Mouginot, J., Morlighem, M., Seroussi, H., and Scheuchl, B.: Widespread, rapid grounding line retreat of Pine Island, Thwaites, Smith, and Kohler glaciers, West Antarctica, from 1992 to 2011, Geophys. Res. Lett., 41, 3502–3509, doi:10.1002/2014GL060140, 2014. 3938
Rolandone, F., Mareschal, J., Jaupart, C., Gosselin, C., Bienfait, G., and Lapointe, R.: Heat flow in the western Superior Province of the Canadian Shield, Geophys. Res. Lett., 30, 2003a. 3946, 3960
Rolandone, F., Mareschal, J.-C., and Jaupart, C.: Temperatures at the base of the Laurentide Ice Sheet inferred from borehole temperature data, Geophys. Res. Lett., 30, doi:10.1029/2003GL018046, 2003b. 3941, 3946, 3952, 3960
Rolandone, F., Jaupart, C., Mareschal, J.-C., Gariépy, C., Bienfait, G., Carbonne, C., and Lapointe, R.: Surface heat flow, crustal temperatures and mantle heat flow in the Proterozoic Trans-Hudson Orogen, Canadian Shield, J. Geophys. Res., 107, doi:10.1029/2001JB000698, 2002. 3960

Sass, J. H., Lachenbruch, A. H., and Jessop, A. M.: Uniform heat flow in a deep hole in the Canadian Shield and its paleoclimatic implications, J. Geophys. Res., 76, 8586–8596, doi:10.1029/JB076i035p08586, 1971. 3940, 3941, 3946, 3960

Schneider, D. P., Steig, E. J., van Ommen, T. D., Dixon, D. A., Mayewski, P. A., Jones, J. M., and Bitz, C. M.: Antarctic temperatures over the past two centuries from ice cores, Geophys. Res. Lett., 33, doi:10.1029/2006GL027057, 2006. 3952

Shen, P. Y. and Beck, A. E.: Determination of surface temperature history from borehole temperature gradients, J. Geophys. Res.-Solid Earth, 88, 7485–7493, doi:10.1029/JB088iB09p07485, 1983. 3944

Shen, P. Y. and Beck, A. E.: Least squares inversion of borehole temperature measurements in functional space, J. Geophys. Res.-Solid Earth, 96, 19965–19979, doi:10.1029/91JB01883, 1991. 3945

Straneo, F. and Heimbach, P.: North Atlantic warming and the retreat of Greenland's outlet glaciers, Science, 504, 36–43, 2013. 3938

Vasseur, G., Bernard, P., de Meulebrouck, J. V., Kast, Y., and Jolivet, J.: Holocene paleotemperatures deduced from geothermal measurements, Palaeogeogr. Palaeoecol., 43, 237–259, doi:10.1016/0031-0182(83)90013-5, 1983. 3944

Velicogna, I. and Wahr, J.: Time-variable gravity observations of ice sheet mass balance: Precision and limitations of the GRACE satellite data, Geophys. Res. Lett., 40, 3055–3063, doi:10.1002/grl.50527, 2013. 3938

Wang, K.: Estimation of ground surface temperatures from borehole temperature data, J. Geophys. Res.-Solid Earth, 97, 2095–2106, doi:10.1029/91JB02716, 1992. 3944

Zwally, H. J., Abdalati, W., Herring, T., Larson, K., Saba, J., and Steffen, K.: Surface Melt-Induced Acceleration of Greenland Ice-Sheet Flow, Science, 297, 218–22, 2002. 3952

Zweck, C. and Huybrechts, P.: Modeling of the northern hemisphere ice sheets during the last glacial cycle and glaciological sensitivity, J. Geophys. Res., 110, 1984–2012, 2005. 3939

Table 1. Technical information concerning the boreholes used in this study.

Site	Log ID	Latitude	Longitude	Depth (m)	λ ($W\,m^{-1}\,K^{-1}$)	Q ($m\,W\,m^{-2}$)	Reference
FlinFlon	n/a	54°43′	102°00′	3196	3.51 (≤ 1920 m) 2.83 (1920–2300 m) 2.51 (≥ 2300 m)	42	Sass et al. (1971)
Thompson – Pipe	01–14	55°29′10″	98°07′42″	1610	3.24	49	Mareschal et al. (1999a); Rolandone et al. (2002); Chouinard and Mareschal (2009)
Thompson – Owl	00–17, 01–16	55°40′17″	97°51′35″	1568	3.0 (< 1200 m) 3.6 (> 1200 m)	52	Mareschal et al. (1999a); Rolandone et al. (2002)
Balmertown	00–02	51°01′59″	93°42′56″	1724	3.3	35	Rolandone et al. (2003a)
Manitouwadge – 0610	06–10	49°09′07″	85°43′46″	2064	2.74	40	Rolandone et al. (2003b); Chouinard and Mareschal (2009)
Manitouwadge – 0611	06–11	49°10′16″	85°46′31″	2279	–	–	Rolandone et al. (2003b); Chouinard and Mareschal (2009)
Sudbury – Victor Mine	13–01	46°40′17″	80°48′34″	2060	2.7	44	
Sudbury – Falconbrige	03–16	46°39′05″	80°47′30″	2122	2.74	47	Perry et al. (2009)
Sudbury – Lockerby	04–01	46°26′00″	81°18′55″	2207	3.29	58	Perry et al. (2009)
Sudbury – Craig Mine	04–02	46°38′34″	81°21′03″	2279	2.65	–	Chouinard and Mareschal (2009)
Val d'Or	10–08	48°06′02″	77°31′26″	1754	3.81	47	Jaupart et al. (2014)
Matagami	04–09	49°42′29″	77°44′28″	1579	3.27 (≤ 1000 m) 4.02 (> 1000 m)	42	
Sept Iles	98-20	50°12′46″	66°38′19″	1820	2.04	32	Mareschal et al. (1999b); Chouinard and Mareschal (2009)

Table 2. Summary of GST history results where T_o is the long-term surface temperature, Q_o is the quasi-equilibrium heat flow, T_{min} is the minimal temperature, T_{pgw} is the maximum temperature attained during the postglacial warming, t_{min} and t_{pgw} is the occurrence of the minimal temperature and maximum postglacial warming temperature. Parentheses indicate sites where the GST history is not reliable.

Site	T_o (°C)	Q_o (m Wm^{-2})	T_{min} (°C)	t_{min} (ka)	T_{pgw} (°C)	t_{pgw} (ka)
FlinFlon	3.8	38.7	−0.25	10–20	5.64	3–5
Pipe	0.7	51.8	0.27	0.15–0.2	–	–
(Owl)[a]	−0.3	54.9	−2.36	5–7.5	2.40	0.9–1
Balmertown	2.6	33.0	1.65	5–7.5	3.36	1–2
Manitouwadge 0610	2.3	35.6	0.95	10–20	3.95	2–3
(Manitouwadge 0611)[b]	1.7	–	−2.83	20–30	6.71	3–5
Victor Mine	4.5	42.1	3.00	10–30	7.34	3–5
Falconbridge	3.1	45.7	−0.20	20–30	5.88	5–7.5
Lockerby	4.1	57.7	2.84	10–30	9.58	3-5
(Craig Mine)[c]	3.0	45.2	−3.20	20–30	8.41	2–3
Val d'Or	2.9	41.9	0.58	10–20	5.33	2–3
Matagami	1.9	47.5	0.34	10–20	4.10	1–2
Sept Iles	2.1	34.7	−1.42	10–20	5.66	1–2

[a] The temperature profile at this site may be distorted by horizontal contrasts in thermal conductivity, [b] The temperature profile in the lowermost part of the hole may be affected by subvertical layering and thermal conductivity contrasts, [c] The temperature profile may be affected by waterflow caused by pumping in the nearby mine.

Table 3. Summary of GST history results for simultaneous inversions where t_{min} and t_{pgw} is the occurrence of the minimal temperature and maximal temperature associated with postglacial warming, and ΔT is the temperature range

Site	ΔT(GSTH) (K)	t_{min} (ka)	t_{pgw} (ka)
Thompson	3.8	5–7.5	1–2
Manitouwadge	7.9	30–40	5–7.5
Sudbury	11.2	30–40	5–7.5
Sudbury (exc. Craig)	6.6	20–30	3–5

Table 4. Ranges in surface temperature variations estimated from: the iteration of the long-term surface temperature as a function of depth (column 1) and from inversion of the GST history (column 2), along with the difference between the two (column 3).

Site	ΔT_o (°C)	ΔT (GSTH) (°C)	Difference
Flin Flon	5.1	6.6	1.5
Thompson, Pipe Mine	5.6	2.5	3.1
Thompson, Owl[a]	5.3	4.8	0.5
Balmertown	2.3	1.7	0.6
Manitouwadge, 0610	3.3	3.0	0.3
Manitouwadge, 0611[b]	9.6	9.5	0.1
Sudbury, Victor Mine	4.9	4.6	0.3
Sudbury, Falconbridge	6.2	7.0	0.8
Sudbury, Lockerby	6.6	6.8	0.2
Sudbury Craig Mine[c]	11.9	11.7	0.2
Val d'Or	5.5	5.2	0.3
Matagami	4.1	3.8	0.3
Sept Iles	7.8	7.1	0.7

[a] The temperature profile at this site may be disturbed by horizontal contrats in thermal conductivity, [b] The temperature profile in the lowermost part of the hole may be affected by subvertical layering and thermal conductivity contrasts, [c] The temperature profile may be affected by waterflow caused by pumping in the nearby mine.

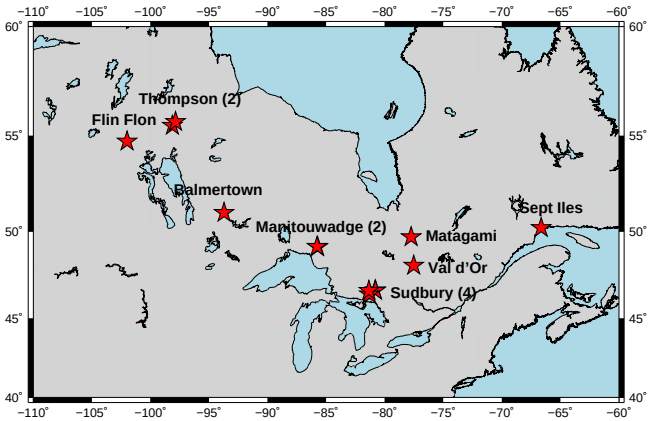

Figure 1. Map of central and eastern Canada and adjoining US showing the location of sampled boreholes. Thompson (Owl and Pipe), Manitouwadge (0610 and 0611) and Sudbury (Falconbridge, Lockerby, Craig Mine, and Victor Mine) have several boreholes present within a small region. The number of profiles available at locations with multiple holes is enclosed in parenthesis.

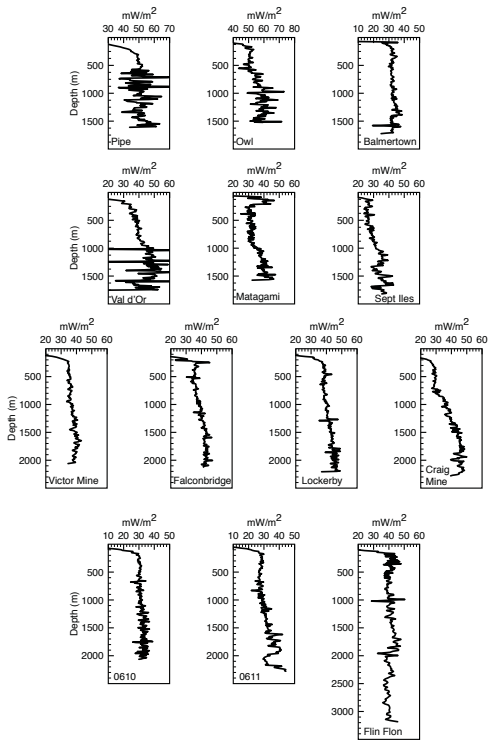

Figure 2. Heat flux variation as a function of depth. The Flin Flon, Owl and Matagami profiles have been corrected to account for thermal conductivity variations with depth as shown in Table 1.

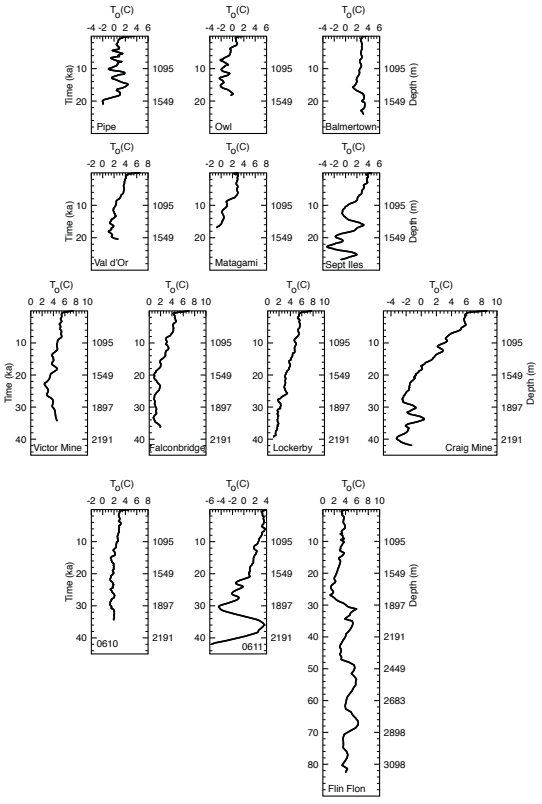

Figure 3. Long-term surface temperature variations over time (left y-axis) and depth (right y-axis) for the boreholes as determined by Eq.6

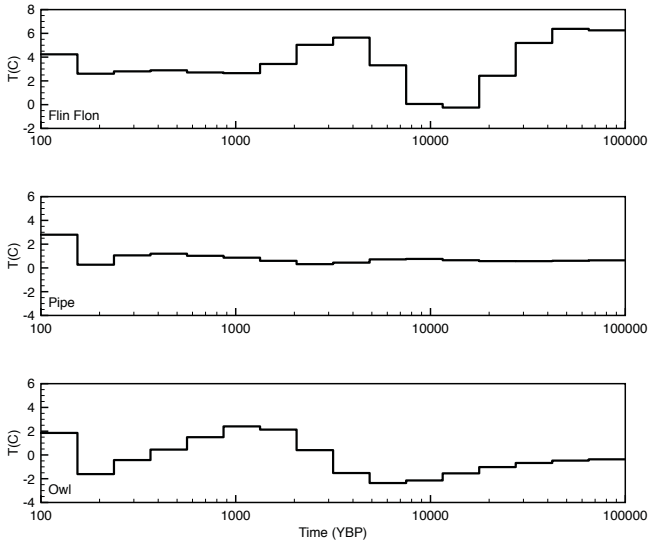

Figure 4. Ground Surface Temperature History from the Manitoba boreholes, at Flin Flon and Thompson (Pipe and Owl). The temperatures have been shifted with respect to the initial surface temperature of the site, T_o, as shown in Table 2.

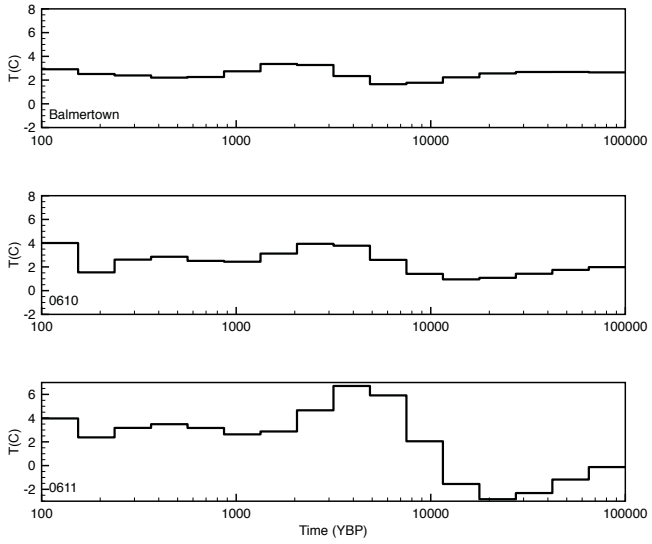

Figure 5. Ground Surface Temperature History for the western Ontario boreholes: Balmertown and Manitouwadge 0610 and 0611. The temperatures have been shifted with respect to the initial surface temperature of the site, T_o, as shown in Table 2.

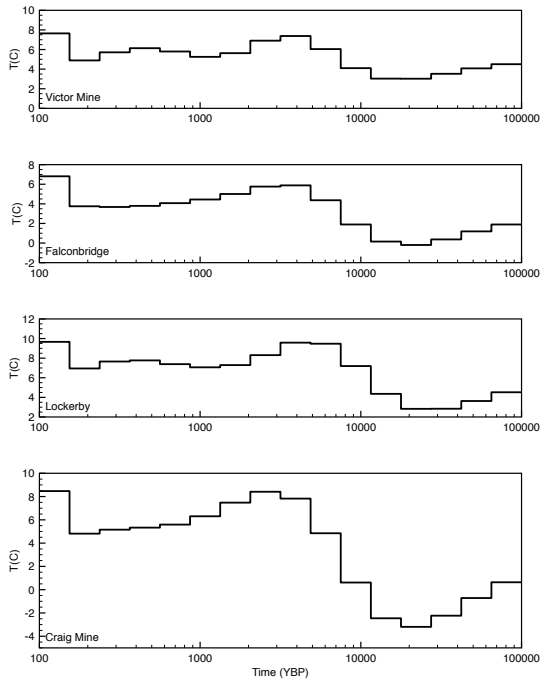

Figure 6. Ground Surface Temperature History for all the boreholes around Sudbury, Ontario (Victor Mine, Falconbridge, Lockerby, and Craig Mine).The temperatures have been shifted with respect to the initial surface temperature of the site, T_o, as shown in Table 2.

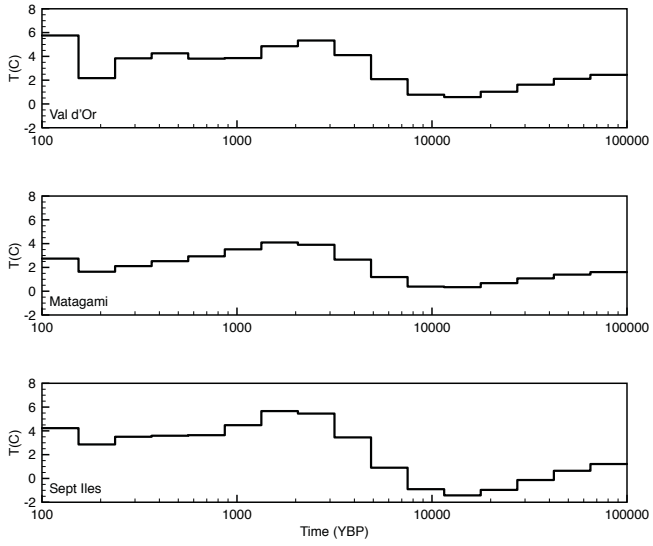

Figure 7. Ground Surface Temperature History for the boreholes in Quebec, Matagami, Val d'Or and Sept-Iles. The temperatures have been shifted with respect to the initial surface temperature of the site, T_o, as shown in Table 2.

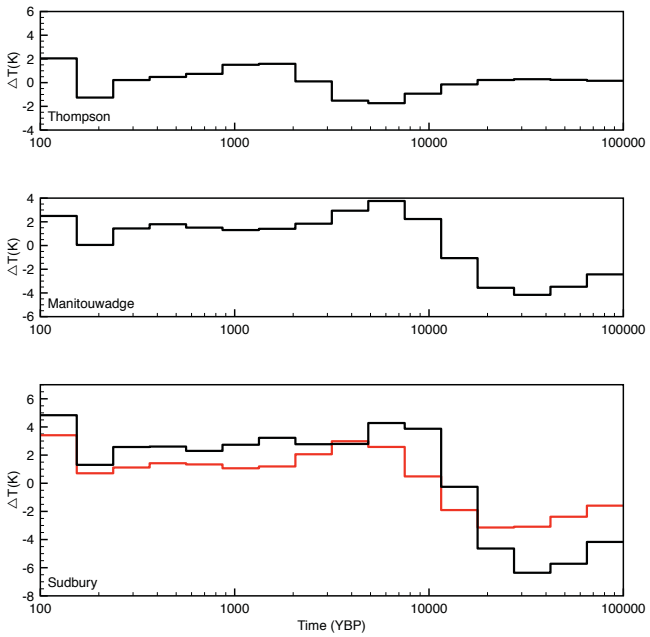

Figure 8. GST changes from simultaneous inversion with respect to the long-term temperature at 100 ka. The Sudbury GST changes include (black) and exclude (red) Craig Mine.